

Surface and bulk photoelectron diffraction from W(110) 4*f* core levels

B. Kim, J. Chen, and J. L. Erskine

Department of Physics, University of Texas, Austin, Texas 78712

W. N. Mei

Department of Physics, University of Nebraska, Omaha, Nebraska 68182

C. M. Wei

Institute of Physics, Academic Sinica, Nankang, Taipei, Taiwan 11529, Republic of China

(Received 15 April 1993)

Energy- and angle-dependent photoelectron cross sections from surface and bulk W(110) 4*f*_{7/2} core levels are measured and compared with dynamical multiple scattering calculations. The agreement between experimental and theoretical results is found to be significantly better than corresponding previous studies, permitting a determination of the first layer atomic plane distance: $d_{12} = 2.26 \pm 0.05$ Å. Forward-scattering enhancements along bond directions are observed under selected scattering conditions. In all cases, final-state multiple scattering accounts for the principal energy and angle dependencies in the cross section. Typical variation of bulk and surface 4*f* photoelectron intensities with kinetic energy or emission angle resulting from final-state effects is observed to be a factor of 2. This result suggests that previous core-level spectra for stepped W(110) surfaces have been incorrectly interpreted.

I. INTRODUCTION

Photoelectron diffraction offers important opportunities as an element-specific probe of surface structure.¹ The most versatile form of the technique requires a tuneable source of soft x-ray photons (energy range extending to a few hundred eV) and a versatile angle-resolving electron energy analyzer capable of measuring the intensity of photoemitted electrons over a wide range of emission angles and kinetic energy. The tuneable photon source permits variation of the kinetic energy of electrons emitted from selected core levels over the energy range where strong diffraction effects occur. The angle-resolving analyzer is used to measure the energy and angle-dependent emission intensities. The energy and angle-dependent electron emission intensities, in principle, contain structural information about the surface, such as bond distances and directions, surface layer separations, and surface reconstruction. These structural parameters must be extracted using appropriate electron-scattering formalisms. At high kinetic energies (500–1000 eV), it has been established that single-scattering formalisms can yield accurate angle-dependent intensity profiles that lead directly to surface structural parameters.² At lower energies (20–500 eV), multiple scattering is known to be very important in governing the diffracted intensity of electrons, and full multiple-scattering formalisms, similar to those used in dynamical low-energy electron-diffraction (LEED) analysis,³ must be employed.

This paper reports photoelectron-diffraction measurements and multiple-scattering analysis for surface and bulk 4*f* core-level cross sections of W(110). It is well established that core-level binding energies of surface atoms are different from those of bulk atoms. The mechanisms responsible for the shifts have been extensively

studied,⁴ and are not of central importance in our present work. What is important is the fact that the shifts are relatively large in certain cases, allowing careful measurements of angle- and energy-dependent diffracted intensities from electrons emitted separately from bulk atoms and from surface atoms. The ability to distinguish between diffracted electrons of essentially the same kinetic energy that originate from bulk or from surface atoms offers an important opportunity for precise evaluation of photoelectron diffraction as a quantitative probe of surface structure.

The W(110) surface offers favorable conditions for experiments devoted to assessing photoelectron diffraction as a structural probe. The surface crystallography is established⁵ [there is no reconstruction as found on the W(100) surface and apparently little or no relaxation], and the second layer 4*f* core-level binding energies appear to be identical to bulk binding energies.⁶ Therefore, there are only two 4*f* peaks (a surface and bulk peak). The surface core-level shift is relatively large (0.3 eV), and the intrinsic linewidths of both the bulk and surface 4*f* core-level peaks are of the same order [0.35-eV full width at half maximum (FWHM)], so that the peaks are easily resolved and their relative intensities can be accurately determined by curve fitting.⁶

II. EXPERIMENT

Our experiments were conducted using the University of Texas at Austin beamline U16A, at the National Synchrotron Light Source, Brookhaven National Laboratory. Radiation from the 750-MeV storage ring was dispersed by a 6-m toroidal grating monochromator,⁷ and photoemitted electrons were analyzed by an angle-resolving hemispherical energy analyzer described previ-

ously.⁸ The angular resolution of all measurements reported here is $\pm 1^\circ$, and the overall energy resolution (monochromator and electron energy analyzer) is 150 meV.

Figure 1 illustrates the geometrical configuration of our experiment and defines the scattering parameters. The following additional parameters are used throughout the paper to describe various measured quantities: KE, kinetic energy of emitted electrons; ϕ_w , surface work function; E_b , binding energy of the bulk $4f_{7/2}$ peaks; and E_s , binding energy of the surface $4f_{7/2}$ peaks. These parameters are related by $KE = h\nu - \phi_w - E_b$ for bulk emission and by the corresponding relation for surface emission.

Our W(110) samples were 1 cm diameter \times 0.1 cm thick, and were cut with surface normal direction within $\pm 1/2^\circ$ of the (110) crystal direction. Standard techniques

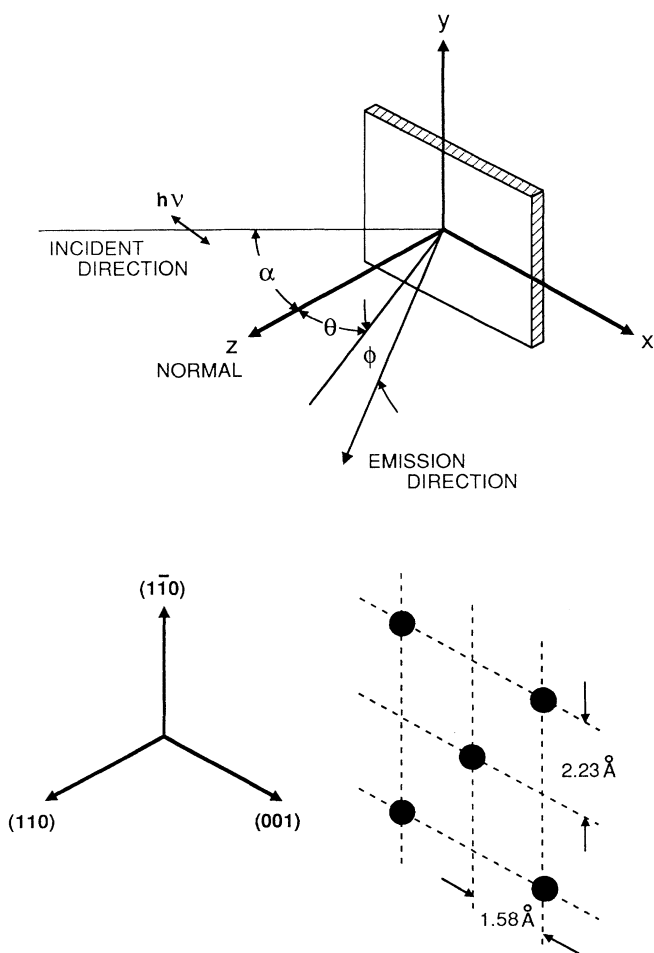


FIG. 1. Upper panel: geometry of experiment. Synchrotron radiation is incident at angle α measured from the surface normal (z direction) with a polarization vector in the x-z plane. Emission angles θ (for emission confined to the xz plane) and θ and ϕ (for emission out of the xz plane) describe the emitted electron direction. Lower panel: crystallographic orientation of the crystal in real space: x direction (001), y direction (010), and z direction (110).

were used to clean the surface: repeated annealing in oxygen to reduce bulk carbon contamination followed by flashing to 2300 K. Surface order was verified by LEED, and surface cleanliness was monitored by Auger electron spectroscopy although the surface-to-bulk ratio of $4f$ core-level intensities was also found to be a good diagnostic probe of surface conditions. All experiments were carried out at pressures below 2×10^{-10} torr, and the sample was flashed frequently during the experiments to maintain a clean surface.

Figure 2 displays a typical set of experimental data and the results of the standard curve-fitting procedure used to extract peak intensities. The two prominent peaks correspond to emission from the W(110) surface ($E_s = 31.15$ eV) and bulk ($E_b = 31.47$ eV) $4f$ core levels. The solid line of the lower electron energy distribution curve (EDC) is a curve-fitting representation of the spectra corresponding to $h\nu = 92$ eV. The normalized residual error (difference between the fit and experimental data divided by \sqrt{N} , where N equals the number of counts) is indicated in a graph below the theoretical curve.

Our curve-fitting procedure is based on an approach developed by Riffe, Wertheim, and Citrin.⁶ The procedure utilizes a five-parameter fit to each line that de-

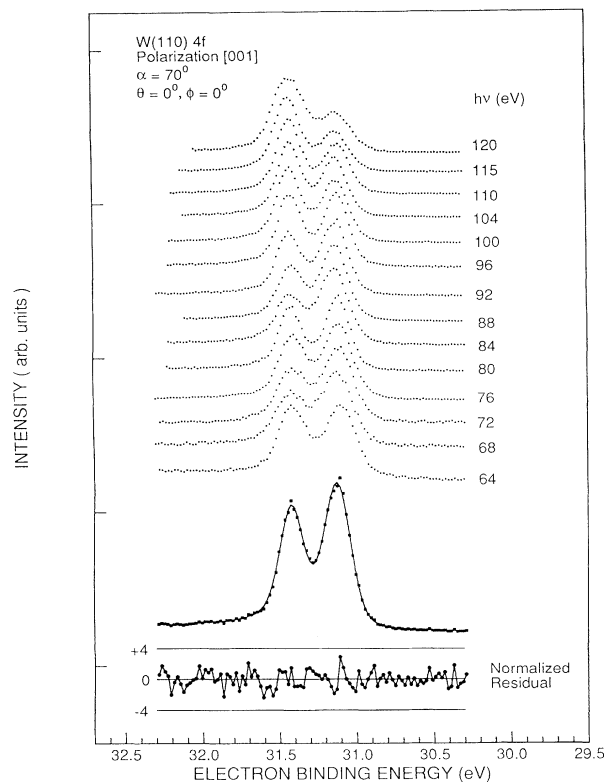


FIG. 2. Sequence of W(110) normal-emission ($\theta = 0$) energy-distribution curves (EDC's), as a function of photon energy indicated at the right of each curve. The angles are defined in Fig. 1. Lower curve, curve-fitting representation of the experimental data for $h\nu = 92$ eV. The normalized residual error (refer to text) is shown below the computer-generated spectra.

scribes the line position (binding energy), amplitude, Lorentzian width (core-hole lifetime), singularity index (conduction-electron screening), and Gaussian width (phonon effects and instrument resolution). While our primary interest in the present work is to obtain accurate relative photoelectron emission cross sections for the bulk and surface $4f$ peaks, the detailed analysis permitted us to compare our experimental results with recent careful work⁶ in which $4f_{7/2}$ line shapes were studied on the W(110) surface. In cases where direct comparisons could be made based on published results, the agreement was found to be excellent.

The background around the bulk and surface core-level peaks was found to vary slightly with scattering parameters. In order to obtain the most accurate surface-to-bulk peak ratios, the background was also fit to an analytical function and subtracted before evaluating the surface and bulk peak areas and ratios. As in the previous studies of surface and bulk W(110) $4f$ line shapes and intensities, which required the careful curve-fitting procedures employed here, certain constraints were imposed on the parameters to ensure that the model was physically meaningful. For example, the Lorentzian widths were chosen to be about 60 and 84 meV, respectively, for the bulk and surface peaks, and the singularity indexes were chosen to be about 0.035 and 0.063 meV for the bulk and surface peaks. The ratios of the Lorentzian widths and of the two singularity indexes were held constant. In fitting most of the spectra, the degrees of freedom (equal to the number of data points minus the number of parameters) is equal to about 180, and the fits yielded chi-square values ranging from 0.85 to 1.15, indicating an accurate fit.

Figure 3 displays photoelectron-diffraction data for W(110) $4f$ surface and bulk excitations. The data are presented in the form of a surface-to-bulk intensity ratio as a function of electron kinetic energy for three scattering configurations. Superimposed on the experimental data are corresponding theoretical results obtained from multiple-scattering calculations described below. The three scattering configurations used to obtain data presented in Fig. 3 were chosen to correspond precisely with those presented by Jugnet *et al.*,⁹ so that a direct comparison can be made (with Fig. 2 of that paper). While there are some similarities between the two data sets, there are many differences—even qualitative dissimilarities. These discrepancies may be a result of different data reduction methods (i.e., curve-fitting procedures), or could be a manifestation of different conditions of the sample surfaces.

III. MULTIPLE-SCATTERING CALCULATIONS

Theoretical calculations of the energy and angle-dependent photoemission cross section of the surface and bulk W $4f$ core levels were performed using a multiple-scattering formalism.¹⁰ The initial state was calculated from a W cluster using the $X\alpha$ scattered-wave method. The final state was described in terms of a multiple-scattering T matrix which propagates the photoelectron through the crystal and out of the surface. Photoelectron

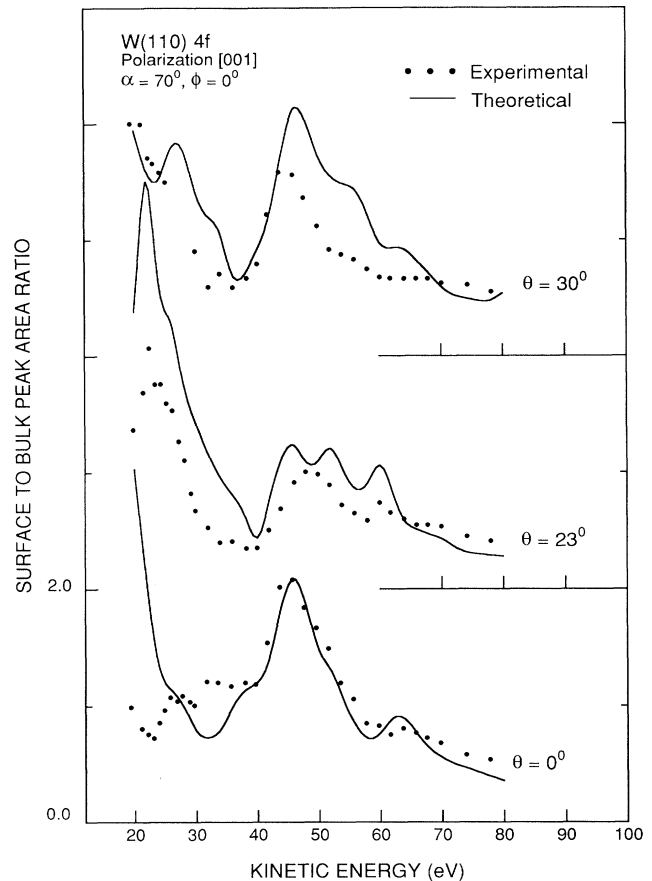


FIG. 3. Reduced experimental data for the W(110) surface-to-bulk intensity ratio as a function of kinetic energy for three polar emission angles $\theta=0^\circ$, 23° , and 30° . Solid curves, corresponding calculation using $d_{12}=d_{\text{BULK}}$ and $V_i=5$ eV.

excitation matrix elements were calculated using the dipole approximation where only the $(l-1)$ and $(l+1)$ channels are included. The binding energy of the W(110) bulk $4f_{7/2}$ core states is 31.47 eV below the Fermi energy. The inner potential, which measures the difference between the kinetic energy of the photoelectron outside and inside the crystal, is chosen to be 18.5 eV to provide the best alignment with experimental data. The potential sensed by the photoelectron was determined by an augmented-plane-wave (APW) calculation which assumes spherical averaging within the muffin-tin approximation.

Phase shifts used to construct the scattering cross section of the bulk and surface atoms were calculated from the band-structure potential.¹¹ The same W phase shifts used in our calculations have been successfully used in a LEED intensity analysis of the structure of one- and two-monolayer epitaxial $p(1\times 1)$ Fe films grown on W(100).¹² In the LEED structure analysis of the Fe layers on W(100),¹² a thorough study of model electron-solid interactions was carried out including an analysis of differences resulting from phase shifts calculated using atomic potentials obtained from both relativistic and nonrelativistic charge densities. In this work, it was

shown that the relativistic and nonrelativistic potentials yield almost identical calculated LEED intensity profiles, both of which correspond well to Feder and Kirschner's¹³ fully relativistic analysis, and adequately to the clean W(001) LEED data.

Photoelectrons emerging from the emitting atom are expressed in terms of spherical waves that are multiply scattered by the surrounding atoms in the same layer. The spherical waves are expanded as plane waves traveling away from the emission layer. The interlayer scatterings are treated by the renormalized forward-scattering method³ which uses the layer reflection as an expansion parameter but sums all of the possible scattering events until numerical convergence is achieved. Inelastic damping and vibrational amplitudes used in the present analysis of W are similar to those in previous work on Ta.¹⁴ The calculation used a fully dynamical multiple-scattering method. Eight partial waves and 81 beams were used in the final-state multiple-scattering calculation. Strong inelastic scattering led to a mean free path of about 4–5 Å at an electron energy of 100 eV, so that only the emission from the first three to four atomic layers significantly contributes to the photocurrent. However, we included the top ten emission layers to ensure convergence. The theoretical surface-to-bulk intensity ratio is calculated by dividing the surface layer emission by the contributions of all the other emitting layers. This ratio is the quantity used to compare with the experimental data that has been reduced to yield the surface-to-bulk intensity ratio. Multilayer relaxation is implemented in the calculation; however, variation of the first interlayer spacing provides the most prominent change in the theoretical curves, and, as discussed below, there appears to be little or no multilayer relaxation of the W(110) surface.

IV. DISCUSSION

Based on the encouraging agreement between our measured and calculated photoelectron-diffraction peak ratios as a function of energy, we carried out corresponding measurements and calculations for a fixed energy and variable angle. Figure 4 presents reduced data and corresponding calculations for a polar angle scan at a photon energy of $h\nu = 136$ eV. The principal features in polar plots of the surface-to-bulk intensity ratio can be understood through simple kinematic arguments. Photoelectron intensity usually reaches a maximum when constructive interference occurs between the direct wave and backscattered waves from the neighboring atoms. The inset of Fig. 4 shows a real-space model of the W(110) crystal as viewed perpendicular to the emission plane. The two major peaks at 20° and 45° result from backscattering along atomic rows (calculated values 18.43° and 45°). The 45° peak corresponds to a string of closely spaced atoms. The diffraction peak is sharp, and the direction is insensitive to energy. The 20° peak results from a more sparsely populated line of atoms. It is weaker, and the shift away from the backscattering angle along with the complicated shape can only accurately be interpreted by using a full multiple-scattering theory.

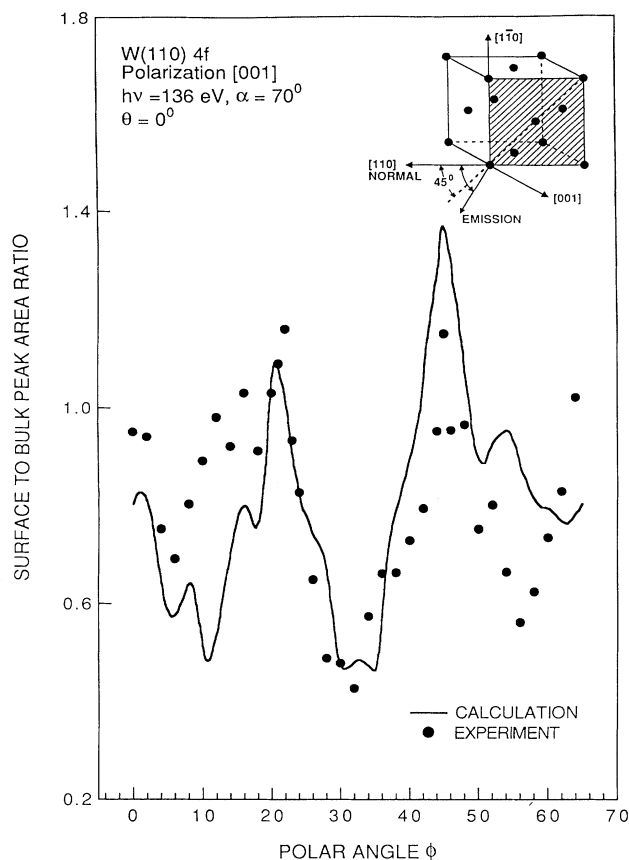


FIG. 4. The polar-angle dependence of the W(110) surface-to-bulk intensity ratio at $h\nu = 136$ eV. The inset shows a cross section of the W(110) lattice in the emission plane. Solid circles, reduced experimental data (refer to discussion of curve fitting); line, theoretical results from multiple-scattering calculation using $d_{12} = d_{\text{BULK}}$ and $V_0 = 5$ eV.

The reasonably good qualitative agreement between experimental and theoretical results presented in Figs. 3 and 4 motivated additional efforts aimed at evaluating the surface structure of W(110) based on our photoelectron diffraction data. Figure 5 summarizes the results. We used standard R -factor analysis (employed in LEED crystallography) to compare the quality of fit between various experimental data sets and theoretical calculations as a function of two parameters— d_{12} , the first layer spacing, and V_0 , the imaginary part of the inner potential that determines the elastic electron mean free path. The best fits (lowest R factors) occurred for $V_i = 5$ eV, and for values of d_{12} very near the bulk value $d_{\text{BULK}} = 2.23$ Å.

Examination of the inset in Fig. 5 shows that the sharpest null in R occurs for the normal-emission data set (one expects that the normal-emission diffraction data should be more sensitive to d_{12} than off-normal data), and that the lowest R factor occurs for d_{12} slightly above the bulk value. Based on our analysis of the photoelectron-diffraction data (refer to R factor plot B in Fig. 5), we obtain $d_{12} = 2.26 \pm 0.05$ Å, in excellent agreement with values established by LEED.⁵

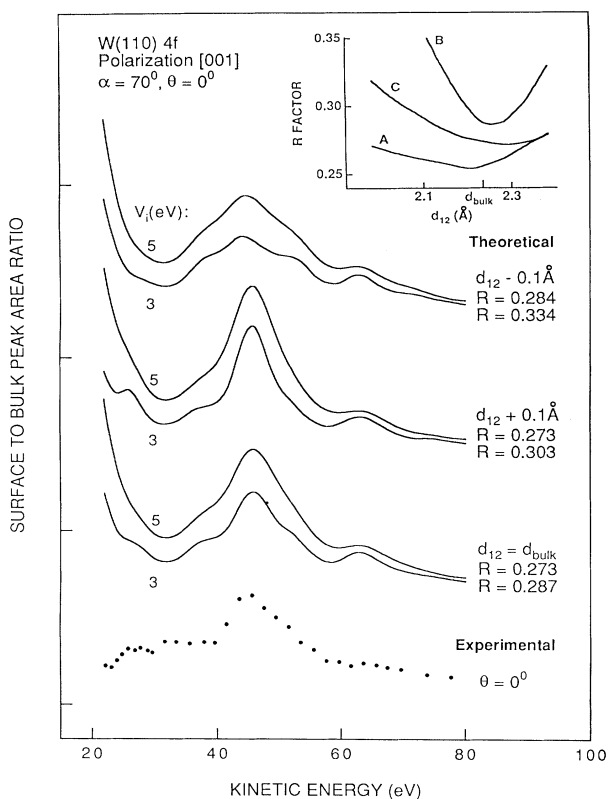


FIG. 5. A comparison of experimental results for $\theta=0$ (lower curve) and calculations for various values of d_{12} and V_i . The best R factors occur for $d_{12} \approx d_{\text{BULK}}$. Inset, variation of d_{12} as a function of data set and parameters: *A*, one set of angle-dependent cross-section data (Fig. 4). *B* and *C*, three sets of energy-dependent cross-section data ($\theta=0^\circ, 23^\circ$, and 30°) with $V_i=3$ and 5 eV, respectively.

Our results have bearing on previous studies of core-level shifts associated with stepped W(110) surfaces.^{15,16} It is well established that one of the factors responsible for shifts in core-level binding energies is the effective atomic coordination. The shift between bulk-atom and surface-atom $4f$ binding energies is readily apparent in Fig. 2, and the typical energy- or angle-dependent intensity modulation resulting from multiple scattering in the final state can be judged from data presented in Figs. 2–4. The maximum experimental modulation of both bulk and surface $4f$ cross sections for W(110) is about a factor of 2, and this result is supported by our multiple-scattering calculations.

Core-level studies of a stepped W(110) surface have been carried out to test initial-state (atomic coordination) models of binding-energy shifts. On stepped surfaces, one expects to observe, in addition to the bulk and surface peaks, new peaks corresponding to step atoms hav-

ing lower coordination than surface atoms, and possibly from other near-step atoms having different coordination from bulk atoms when coordination out to third-nearest neighbors is considered.

Core-level spectra for various stepped W(110) surfaces^{15,16} are indeed found to manifest differences compared to corresponding spectra for flat W(110). Curve fitting must be employed to interpret the results because the various peaks overlap. However, our results for W(110) suggest that incorrect analysis has been carried out on spectra from the stepped W surfaces. For example, examination of Fig. 5 of Ref. 15 reveals that the assigned binding energy of $4f$ emission from step atoms is based on a curve-fitting procedure that requires the bulk-atom cross section to change by over a factor of 10 between $h\nu=85$ and 95 eV. Similarly, the surface-atom cross section must also change by over a factor of 10 between $h\nu=75$ and 80 eV. These changes are unrealistic based on our results. A more realistic model of core-level shifts on stepped W(110) surfaces will be discussed in a future publication.¹⁷

V. CONCLUSIONS

Our photoelectron-diffraction data for W(110) $4f$ surface and bulk core levels depart significantly from previous measurements.⁹ Our multiple-scattering analysis of the corresponding surface and bulk photoelectron-diffraction intensities are in good agreement with the previous calculations⁹ and with our own experimental results. Using R -factor analysis techniques, we have obtained an accurate independent evaluation of the top interlayer spacing for W(110). We find the top interlayer spacing essentially unrelaxed from the bulk value, in excellent agreement with a previous LEED study.⁵ We conclude that measurements of the surface-to-bulk photoelectron-diffraction ratio from core levels offer suitable sensitivity for accurate quantitative surface structural analysis. In addition, the modulation of $4f$ photoelectron intensity resulting from multiple-scattering final-state effects is found to be of the order of a factor of 2 for both energy-dependent and angle-dependent measurements. Since the interpretation of previous $4f$ core-level spectra¹⁵ on stepped W(110) surfaces is based on emission amplitude changes exceeding a factor of 10 for surface and bulk peaks, it appears that these spectra have been incorrectly interpreted.

ACKNOWLEDGMENTS

Two of the authors (W.N.M. and C.M.W.) would like to thank Professor S. Y. Tong for stimulating discussions and the hospitality extended to them during their stays at the University of Wisconsin at Milwaukee. This work was supported by NSF DMR89-22359 and the Robert A. Welch Foundation. The National Synchrotron Light Source is supported by the U.S. DOE.

- ¹D. P. Woodruff, D. Norman, B. W. Holland, N. V. Smith, H. H. Ferrell, and M. M. Traum, *Phys. Rev. Lett.* **41**, 1130 (1978); S. D. Kevan, R. F. Davis, D. H. Rosenblatt, J. G. Tobin, M. G. Mason, D. A. Shirley, C. H. Li, and S. Y. Tong, *ibid.* **46**, 1629 (1981); K.-U. Weiss, R. Dippel, K.-M. Schindler, P. Gardner, V. Fritzsche, A. M. Bradshaw, A. L. D. Kilcoyne, and D. P. Woodruff, *ibid.* **69**, 3196 (1992).
- ²W. F. Egelhoff, Jr., *Crit. Rev. Solid State Mater. Sci.* **16**, 213 (1990).
- ³M. A. Van Hove and S. Y. Tong, *Surface Crystallography by LEED* (Springer-Verlag, Berlin, 1979).
- ⁴T.-C. Chiang, *CRC Crit. Rev. Solid State Mater. Sci.* **14**, 269 (1988); D. Spanjaard, C. Guillot, G. Treglia, and J. Lecante, *Surf. Sci. Rep.* **5**, 1 (1985).
- ⁵M. K. Debe and D. A. King, *Surf. Sci.* **81**, 193 (1979).
- ⁶D. M. Riffe, G. K. Wertheim, and P. H. Citrin, *Phys. Rev. Lett.* **63**, 1976 (1989).
- ⁷L. H. Breaux and J. L. Erskine, *Nucl. Instrum. Methods A* **246**, 248 (1986).
- ⁸H. A. Stevens, A. M. Turner, A. W. Donoho, and J. L. Erskine, *J. Electron Spectrosc. Relat. Phenom.* **32**, 327 (1983).
- ⁹Y. Jugnet, N. S. Prakash, L. Porte, T. M. Duc, T. T. A. Nguyen, R. Cinti, H. C. Poon, and G. Grenet, *Phys. Rev. B* **37**, 8066 (1988).
- ¹⁰C. H. Li, A. R. Lubinsky, and S. Y. Tong, *Phys. Rev. B* **17**, 3128 (1978).
- ¹¹L. F. Matheiss, *Phys. Rev.* **139**, 236 (1965).
- ¹²M. Drakaki, J. Chen, J. L. Erskine, C. B. Duke, and A. Paton (unpublished).
- ¹³R. Feder and J. Kirschner, *Surf. Sci.* **103**, 75 (1981).
- ¹⁴R. A. Bartynski, D. Heskett, K. Garrison, G. M. Watson, D. M. Zehner, W. N. Mei, S. Y. Tong, and X. Pan, *Phys. Rev. B* **40**, 5340 (1989).
- ¹⁵D. Chauveau, P. Roubin, C. Guillot, J. Lecante, G. Treglia, M. C. Desjonqueres, and D. Spanjaard, *Solid State Commun.* **52**, 635 (1984).
- ¹⁶K. G. Purcell, J. Jupille, and D. A. King, *Surf. Sci.* **208**, 245 (1989).
- ¹⁷D. M. Riffe, B.-S. Kim, J. L. Erskine, and N. D. Shinn (unpublished).